

Evaluation of radioiodinated 5-iodo-3-(2(*S*)-azetidylmethoxy)pyridine as a ligand for SPECT investigations of brain nicotinic acetylcholine receptors

Hideo SAJI, Mikako OGAWA, Masashi UEDA, Yasuhiko IIDA, Yasuhiro MAGATA, Akiko TOMINAGA, Hidekazu KAWASHIMA, Youji KITAMURA, Masaki NAKAGAWA, Yasushi KIYONO and Takahiro MUKAI

Graduate School of Pharmaceutical Sciences and Graduate School of Medicine, Kyoto University

5-Iodo-3-(2(*S*)-azetidylmethoxy)pyridine (5IA), an A-85380 analog iodinated at the 5-position of the pyridine ring, was evaluated as a radiopharmaceutical for investigating brain nicotinic acetylcholine receptors (nAChRs) by single photon emission computed tomography (SPECT). [$^{123/125}\text{I}$]5IA was synthesized by the iododestannylation reaction under no-carrier-added conditions and purified by high-performance liquid chromatography (HPLC) with high radiochemical yield (50%), high radiochemical purity (> 98%), and high specific radioactivity (> 55 GBq/ μmol). The binding affinity of 5IA for brain nAChRs was measured in terms of displacement of [^3H]cytisine and [^{125}I]5IA from binding sites in rat cortical membranes. The binding data revealed that the affinity of 5IA was the same as that of A-85380 and more than seven fold higher than that of (–)-nicotine, and that 5IA bound selectively to the $\alpha 4\beta 2$ nAChR subtype. Biodistribution studies in rats indicated that the brain uptake of [^{125}I]5IA was rapid and profound. Regional cerebral distribution studies in rats demonstrated that the accumulation of [^{125}I]5IA was consistent with the density of high affinity nAChRs with highest uptake observed in the nAChR-rich thalamus, moderate uptake in the cortex and lowest uptake in the cerebellum. Administration of the nAChR agonists (–)-cytisine and (–)-nicotine reduced the uptake of [^{125}I]5IA in all regions studied with most pronounced reduction in the thalamus, and resulted in similar levels of radioactivity throughout the brain. [^{125}I]5IA binding sites were shown to be saturable with unlabeled 5IA. Behavioral studies in mice demonstrated that 5IA did not show signs of behavioral toxicity. Furthermore, SPECT studies with [^{123}I]5IA in the common marmoset demonstrated appropriate brain uptake and regional localization for a high-affinity nAChR imaging radiopharmaceutical. These results suggested that [^{123}I]5IA is a promising radiopharmaceutical for SPECT studies of central nAChRs in human subjects.

Key words: 5-iodo-3-(2(*S*)-azetidylmethoxy)pyridine, radioiodination, nicotinic acetylcholine receptor, brain, single photon emission computed tomography

INTRODUCTION

CHANGES IN THE DENSITY of nicotinic acetylcholine receptors (nAChRs) have recently been reported in the brains of patients with various disorders, including Alzheimer's disease and Parkinson's disease.^{1–10} An increased den-

sity of nicotine receptors has also been reported in the brains of smokers.^{11–13} In addition, evidence of an important role of nAChRs in cognition and improvement of cognitive function by nicotine have been reported.^{14–18} These observations and the superior radiation properties of ^{123}I for single photon emission computed tomography (SPECT) prompted us to develop a radioiodinated ligand that is suitable for *in vivo* imaging. Therefore, based on structure-activity relationship studies of nicotine, we developed (–)-5-iodonicotine, a (–)-nicotine analog iodinated at the 5-position of the pyridine ring.^{19,20} *In vitro* receptor binding and *in vivo* biodistribution studies of this compound showed that the binding affinity for nAChRs

Received August 13, 2001, revision accepted January 16, 2002.

For reprint contact: Hideo Saji, M.D., Graduate School of Pharmaceutical Sciences, Kyoto University, Yoshida Shimoadachi-cho, Sakyo-ku, Kyoto 606–8501, JAPAN.

E-mail: hsaji@pharm.kyoto-u.ac.jp

was the same as that of (–)-nicotine, the parent compound, and deiodination *in vivo* was minimized. These results indicated that position 5 of the pyridine ring of (–)-nicotine was the most practical site for iodination from the viewpoints of minimum disturbance of receptor binding and maximum *in vivo* stability, but its usefulness was significantly impaired by high nonspecific uptake and rapid clearance from the brain. Impetus for further work on the development of a radioligand for *in vivo* imaging of nAChRs has been provided by the discovery of epibatidine, an alkaloid from the skin of the poisonous Ecuadorian frog *Epipedobatus tricolor* with extremely high affinity for nAChRs in the brain.^{21–31} The radioiodinated epibatidine derivative, (±)-exo-2-(2-[¹²³I]iodo-5-pyridyl)-7-azabicyclo[2.2.1]heptane (IPH) has been synthesized and shown to be a highly specific and selective nAChRs ligand with favorable brain accumulation and kinetics.^{30,31} But IPH displayed a narrow safety margin as it produced catecholamine release and pronounced cardiovascular effects at a very low dose of approximately 30 times that needed for *in vivo* imaging.²⁹ More recently, 3-[2(*S*)-2-azetidylmethoxy]pyridine (A-85380) has been developed, which has high affinity comparable to that of epibatidine at nAChRs but with much less toxicity.³² The favorable properties for *in vivo* nAChR imaging therefore prompted us to synthesize a radioiodinated A-85380 analog.

The selection of the site introduced radioiodine is important for the development of a radioiodinated nAChR imaging agent, as demonstrated in design of (–)-5-iodonicotine.^{19,20} With regard to the nicotinic pharmacophore, the recently developed model suggests that the binding of nicotine to nAChRs is associated with a pyrrolidine nitrogen atom (a cationic center), a pyridine nitrogen atom (an electronegative atom), planarity of the pyridine ring (a dummy point or an atom to define a line along which the hydrogen bond may form), and the distance between the two nitrogen atoms.^{32–35} Therefore, when a cationic center, a pyridine nitrogen atom and planarity of the pyridine ring were selected as essential

pharmacophoric elements and A-85380 was superimposed on (–)-5-iodonicotine, the position of iodine in (–)-5-iodonicotine was superimposed on position 5 of the 3-pyridyl fragment in A85380 as shown in Figure 1. Therefore, since (–)-5-iodonicotine showed the same affinity as (*S*)-nicotine without disturbance of receptor binding, it has been suggested that the 5 position of the 3-pyridyl fragment is the best site for iodination in A-85380.

In fact, Koren et al. recently synthesized all of the A-85380 derivatives iodinated at possible positions of the 3-pyridyl fragment, that is 2-, 4-, 5- and 6-iodinated derivatives of A-85380 and found that an A-85380 derivative iodinated at the 5 position of the 3-pyridyl fragment, 5-iodo-3-(2(*S*)-azetidylmethoxy)pyridine (5IA), had the highest affinity for nAChRs among all synthesized derivatives.³⁶ Furthermore, they performed biodistribution studies in mice and SPECT image studies in baboons, and suggested that [¹²³I]5IA is a promising SPECT imaging agent of nAChRs.^{37–41}

In this study, to evaluate the applicability of [¹²³I]5IA to the clinical nuclear medical imaging studies of neuronal nAChR, 5IA was synthesized and its *in vitro* receptor binding affinity and selectivity, biodistribution in rats including regional cerebral distribution, acute toxicity and imaging with SPECT in the common marmoset were investigated. A part of this work was presented at the 119th meeting of The Pharmaceutical Society of Japan, held in 1999 (Tokushima).

MATERIALS AND METHODS

Sodium [¹²⁵I]iodide (specific activity: 81.4 GBq/μmol) and [³H](–)-cytisine (1.13 TBq/mmol) were purchased from Amersham International, Plc. Ammonium [¹²³I]iodide produced by the indirect method with ¹²⁴Xe (*p,2n*) ¹²³Cs and/or ¹²⁴Xe (*p,pn*) ¹²³Xe reactions was obtained from Nihon Medi-Physics Co. Ltd. (specific activity : 8.88 TBq/μmol). All other chemicals used were of reagent grade. Male Wistar rats were supplied by Japan SLC Co. Ltd. (Hamamatsu, Japan) and a male common marmoset (*Callithrix jacchus*) was obtained from Sumitomo Chemical Co. Ltd. (Osaka, Japan). The animal studies were conducted in accordance with our institutional guidelines and approved by Kyoto University Animal Care Committee.

Synthesis of 5-iodo-3-(2(*S*)-azetidylmethoxy)pyridine (5IA)

5IA was synthesized according to the methods of Koren et al. and Musachio et al.^{36,40} Briefly, the procedures for preparation of 5IA are described below (Fig. 2).

(*S*)-1-(tert-Butoxycarbonyl)-2-azetidine-2-carboxylic acid (2)

To an ice-cold solution of (*S*)-2-azetidincarboxylic acid (1) (600 mg, 5.94 mmol) in 1,4-dioxane : water (18 ml,

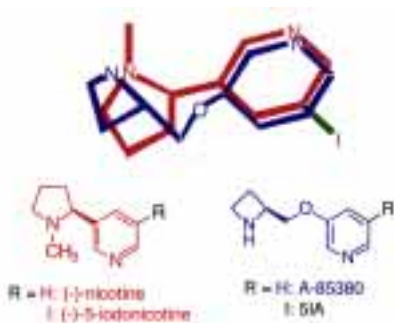


Fig. 1 Chemical structures of 5-iodo-3-(2(*S*)-azetidylmethoxy)pyridine (5IA) and related compounds and superposition of A-85380 on (–)-5-iodonicotine.

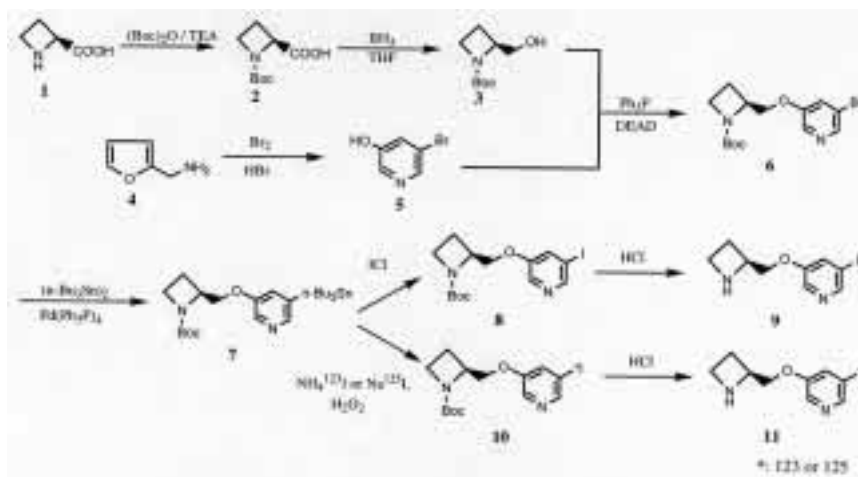


Fig. 2 Synthesis of unlabeled 5IA and [^{123/125}I]5IA.

1 : 1) was added di-*tert*-butyl dicarbonate (1.69 g, 7.72 mmol) at 0°C, followed by triethylamine (952 μ l, 6.83 mmol). The reaction mixture was stirred for 18 h, with gradual warming to room temperature. **2** was yielded as a white semisolid by extraction with ethyl acetate (1.16 g, 97% yield). ¹H-NMR (CDCl₃): 1.48 (s, 9H), 2.37–2.60 (m, 2H), 3.99–3.83 (m, 2H), 4.78–4.84 (t, 1H). FAB MS m/z: 202 (M + H)⁺.

(S)-1-(*tert*-Butoxycarbonyl)-2-azetidinemethanol (**3**)

To a solution of the compound **2** (1.97 g, 9.82 mmol) in tetrahydrofuran (THF) (21 ml) was added borane/THF complex (1M, 10 ml, 4.5 equiv.) at 0°C under an argon atmosphere. The mixture was allowed to gradually warm to room temperature and was stirred for 48 h. **3** was yielded as a colorless oil by extraction with ethyl acetate (1.65 g, 90% yield). ¹H-NMR (CDCl₃): 1.45 (s, 9H), 1.96–2.12 (m, 1H), 2.14–2.27 (m, 1H), 3.72–3.92 (m, 4H), 4.43 (m, 1H).

3-Hydroxy-5-bromopyridine (**5**)

Over a period of 5 h, 5.5 ml (0.108 mol) of bromine was added dropwise to a solution of 0.05 mol (4.86 g) of 2-furfurylamine (**4**) in 21.7 g of 11.5% hydrobromic acid (0.031 mol) at –12°C. The solution was subsequently stirred under nitrogen for 17 h at –20°C. After a stream of nitrogen was passed through the resulting solution, the solution obtained was brought to pH 1, followed by refluxing for 5 min at 130°C. **5** was yielded as a white powder by recrystallizing from toluene (1.29 g, 15% yield). ¹H-NMR (CDCl₃): 7.43–7.44 (t, 1H), 8.18–8.19 (d, 1H), 8.23–8.24 (d, 1H). FAB MS m/z: 174, 176 (M + H)⁺. *Anal.* Calcd for C₅H₄NOBr: C, 34.51; H, 2.32; N, 8.05. Found: C, 36.33; H, 2.71; N, 8.26.

5-Bromo-3-((S)-1-(*tert*-butoxycarbonyl)-2-azetidinylmethoxy)pyridine (**6**)

To a solution of compound **3** (1.1 g, 5.7 mmol) in THF (30

ml) was added diethyl azodicarboxylate (3.9 ml, 8.5 mmol) at 0°C under an argon atmosphere, followed by triphenylphosphine (2.2 g, 8.5 mmol). After 10 min, compound **5** (1.5 g, 8.5 mmol) was added to the reaction mixture and stirred for 40 h. **6** was yielded as a colorless oil by purification by flash silica gel column chromatography (0.73 g, 37% yield). ¹H-NMR (CDCl₃): 1.43 (s, 9H), 2.25–2.42 (m, 2H), 3.90 (t, 2H), 4.12 (dd, 1H), 4.32–4.33 (m, 1H), 4.51–4.53 (m, 1H), 7.43–7.44 (t, 1H), 8.29 (m, 2H). FAB MS m/z: 343, 346 (M + H)⁺. *Anal.* Calcd for C₁₄H₁₉N₂O₃Br: C, 48.99; H, 5.58; N, 8.16. Found: C, 48.90; H, 5.66; N, 8.30.

5-(Tri-*n*-butylstannyl)-3-((S)-1-(*tert*-butoxycarbonyl)-2-azetidinylmethoxy)pyridine (**7**)

Compound **6** (500 mg, 1.46 mmol) and hexa-*n*-butylditin (2.11 g, 3.64 mmol) were dissolved in dry toluene (4 ml), and a catalytic amount of tetrakis(triphenylphosphine) palladium (16.8 mg, 0.015 mmol) was added. The mixture was refluxed with stirring for 18 h under an argon atmosphere. **7** was yielded as a colorless oil by purification by silica gel column chromatography (0.47 g, 58%). ¹H-NMR (CDCl₃): 0.86–1.59 (m, 36H), 2.00–2.05 (m, 1H), 2.26–2.39 (m, 2H), 3.90 (dd, 2H), 4.15 (dd, 1H), 4.32 (dd, 1H), 4.52–4.54 (m, 1H), 7.28–7.30 (dd, 1H), 8.21 (dd, 1H), 8.23 (dd, 1H). FAB-MS m/z: 553, 555 (M + H)⁺. *Anal.* Calcd for C₂₆H₄₆N₂O₃Sn: C, 56.43; H, 8.38; N, 5.06. Found: C, 56.23; H, 8.54; N, 5.16.

5-Iodo-3-((S)-1-(*tert*-butoxycarbonyl)-2-azetidinylmethoxy)pyridine (**8**)

A solution of iodine monochloride (11 mg, 0.068 mmol) in 10 ml of chloroform was added dropwise to a stirred suspension of **7** (31.2 mg, 0.056 mmol) in chloroform (2 ml). The reaction mixture was stirred at ambient temperature for an additional 1h and yielded **8** as a colorless oil. ¹H-NMR (CDCl₃): 1.43 (s, 9H), 2.28–2.35 (m, 2H), 3.90 (t, 2H), 4.09–4.13 (dd, 1H), 4.31–4.32 (m, 1H), 4.50–4.52

(m, 1H), 7.60–7.61 (dd, 1H), 8.29–8.30 (d, 1H), 8.43 (d, 1H).

5-Iodo-3-(2(S)-azetidinylmethoxy)pyridine dihydrochloride (5IA) (9)

To a solution of compound **8** (107 mg, 0.27 mmol) in absolute ethanol (3.5 ml) at 0°C under an argon atmosphere was added a saturated solution of hydrogen chloride in ethanol (3.5 ml). The reaction mixture was stirred for 4.5 h while gradually warming to room temperature. The resulting white powder was obtained by filtration, and washed with ethyl ether, yielding **9** (10.6 mg, 11% yield) as a white powder. ¹H-NMR (D₂O): 2.72 (dd, 2H), 4.07–4.22 (m, 2H), 4.50 (d, 2H), 4.80–4.84 (m, 1H), 4.95–5.01 (m, 1H), 4.32 (dd, 1H), 4.52–4.54 (m, 1H), 8.35 (d, 1H), 8.50 (d, 1H), 8.65 (d, 1H). FAB-MS *m/z*: 291 C₉H₁₁N₂OI (M + H)⁺. *Anal.* Calcd for C₉H₁₁N₂OI·2HCl: C, 29.78; H, 3.61; N, 7.72. Found: C, 29.30; H, 3.53; N, 7.53.

Radiosynthesis of [¹²⁵I]5IA and [¹²³I]5IA (II)

[¹²⁵I]5IA

To a mixture of sodium [¹²⁵I]iodide was added compound **7** (0.1 mg in ethanol), 1.5% aqueous acetic acid and 30% aqueous hydrogen peroxide, and the mixture was stirred for 30 min at room temperature. Concentrated hydrochloric acid was then added, and stirred for 5 min at room temperature. The mixture was then basified with 3N sodium hydroxide, the product was extracted with ethyl acetate, and the combined organic layers were evaporated. The residue was dissolved in methanol, and purified by reverse-phase HPLC [Cosmosil 5C₁₈-300 10 × 250 mm, Nacalai Tesque, Kyoto, Japan, eluted with methanol: 10 mM ammonium acetate : triethylamine (375 : 376 : 1) at a flow rate of 1.5 ml/min (t_R = 40 min for [¹²⁵I]5IA)].

[¹²³I]5IA

After an ammonium [¹²³I]iodide solution was heated and the solvent was removed, compound **7** (0.1 mg in ethanol), 1.5% aqueous acetic acid, 3N hydrochloric acid and 30% aqueous hydrogen peroxide were added to a vial and stirred for 30 min at 60°C. To the resulting solution was added concentrated hydrochloric acid, followed by stirring for 5 min at 60°C. The mixture was then basified with 3N sodium hydroxide, the product was extracted with ethyl acetate, and the combined organic layers were evaporated. The residue was purified by the same procedure as described for [¹²⁵I]5IA by HPLC.

Preparation of rat brain synaptosomes

Preparation of synaptosomal membranes from the rat cortex, thalamus, striatum, superior colliculus and cerebellum were carried out according to the method of Pabreza et al. with slight modifications.⁴² Briefly, each tissue sample from male Wistar rats (230 g) was homogenized in 50 mM Tris-HCl buffer (pH 7.4) containing 120

mM NaCl, 5 mM KCl, 1 mM MgCl₂, and 2.5 mM CaCl₂ with a Polytron. The homogenates were then centrifuged at 45,000 × *g* for 10 min at 4°C, and the pellets resuspended in fresh buffer to yield a synaptosomal membrane suspension with a protein concentration of 10 mg/ml. The protein concentration was measured by the method of Lowry et al.⁴³

Inhibition of [³H]cytisine and [¹²⁵I]5IA binding to rat cortical membranes by various drugs

Aliquots of 100 μl of the cortical membrane preparation (1 mg protein) were incubated at 2°C with various concentrations of competing drugs and the radioligand (5 nM [³H](–)-cytisine or 0.6 nM [¹²⁵I]5IA) in 0.15 ml of 50 mM Tris-HCl buffer (pH 7.4) containing 120 mM NaCl, 5 mM KCl, 1 mM MgCl₂, and 2.5 mM CaCl₂. When acetylcholine was used in competition studies, 200 μM diisopropyl fluorophosphate, a cholinesterase inhibitor, was added to the tissue homogenate approximately 30 min before starting the assay. Incubation was performed for 75 min at 2°C, after which the samples were rapidly filtered through polylysine-soaked Whatman GF/C filters, and the filters were washed rapidly three times with 4 ml of ice-cold assay buffer. For [³H](–)-cytisine, the filter was placed in a 20-ml scintillation vial containing 10 ml of ACS II (Amersham), and the radioactivity bound to the filter was counted. For [¹²⁵I]5IA, the radioactivity bound to the filter was measured in a NaI well scintillation counter. Nonspecific binding was determined in the presence of 1 mM (–)-nicotine. The IC₅₀ values were determined from displacement curves of the percent inhibition of [³H](–)-cytisine or [¹²⁵I]5IA binding *versus* the inhibitor concentration by means of the LIGAND curve-fitting computer program (Elsevier-Biosoft, Cambridge, U.K.). K_i values were calculated by the method of Cheng and Prusoff.⁴⁴ To calculate K_i, the value of 0.96 nM reported by Pabreza et al. was used as the K_D for cytisine,⁴² and the value obtained in this study (0.22 nM) was used as the K_D for 5IA.

Biodistribution studies

Male Wistar rats weighing about 230 g were injected via the tail vein with [¹²⁵I]5IA (111 kBq) in 0.2 ml of ethanolic saline solution (< 0.5% ethanol). At the designated time points after injection, the rats were killed by decapitation and their organs were removed. The tissues were then weighed and the radioactivity was counted in a NaI well scintillation counter.

The relative binding affinity of [¹²⁵I]5IA for nicotinic acetylcholine receptors was determined with various drugs, which were injected into rats given 111 kBq of [¹²⁵I]5IA. (–)-Cytisine (1 mg/kg), (–)-nicotine (60 μg/kg), (+)-nicotine (0.3 mg/kg), dexetimide (10 mg/kg) and 5IA (0.1 mg/kg) were injected intravenously 5 min before the radioligand, and scopolamine (10 mg/kg) and mecamilamine (5 mg/kg) were injected subcutaneously 30 min

before the radioligand. The rats were killed 60 min after radioligand administration. The brain regions were dissected and the radioactivity was counted.

Ex vivo autoradiographic studies

Two groups of male Wistar rats weighting about 250 g were used. One group was intravenously injected with 1.7 MBq of [¹²⁵I]5IA, and the other group received the same dose of [¹²⁵I]5IA 5 min after intravenous injection of (–)-cytisine (1 mg/kg). At 60 min after radioligand injection, the rats were decapitated, and their brains were quickly removed, frozen, and cut into sections 20 μm thick with a cryomicrotome. The sections were thaw-mounted on gelatin-coated slides, which were then placed on autoradiography film (Hyperfilm-³H type, Amersham) for 8 days along with calibrated ¹²⁵I-labeled external standards ([¹²⁵I]Microscales, Amersham).

Metabolic studies

Male Wistar rats weighing about 230 g were injected intravenously with 111 kBq of [¹²⁵I]5IA and then decapitated 60 min after injection. The brains were removed immediately and homogenized in 2 ml of methanol. After centrifugation at 1,750 × g for 10 min at 4°C, the precipitate was washed with 1 ml of methanol and the wash was combined with the supernatant. The combined methanol extracts were evaporated under a stream of nitrogen to a small volume, and analyzed by HPLC on a Cosmosil 5C₁₈-300 column (10 × 250 mm, Nacalai Tesque, Kyoto, Japan) eluted with methanol : 10 mM ammonium acetate (45 : 55) at a flow rate of 1.5 ml/min (t_R = 22 min for [¹²⁵I]5IA). The blood samples were collected in heparinized tubes and centrifuged at 1,000 × g for 10 min at 4°C to collect plasma samples. These plasma samples were extracted twice with 2 ml of methanol, and the combined methanol extracts were analyzed by HPLC as described above.

Determination of the brain uptake Index (BUI)

The BUI values for [¹²⁵I]5IA and [³H]nicotine were determined by the method of Oldendorf.⁴⁵ A mixture of 200 μl of saline containing the labeled compounds (37 kBq) and [¹⁴C]butanol was injected into the right common carotid artery of male Wistar rats (250 g) and the rats were killed by decapitation 15 sec after injection. Part of the cortex was removed from each rat and the ¹²⁵I radioactivity (A) was counted in a NaI well scintillation counter. The samples were then treated with NCS tissue solubilizer (Amersham) and the ³H or ¹⁴C radioactivity (B) was counted in a liquid scintillation counter. In the case of ¹²⁵I-labeled compounds, the radioactivity of suitably diluted aliquots of the injected sample was also counted in both a NaI well scintillation counter (C) and a liquid scintillation counter (D), and the ¹⁴C radioactivity of the brain tissue was determined as follows: ¹⁴C radioactivity = B – (A × D/C). Finally, the BUI was calculated with the following

formula:

$$\text{BUI} = \frac{^{125}\text{I or } ^3\text{H in brain}/^{14}\text{C in brain}}{\text{Injected } ^{125}\text{I or } ^3\text{H}/\text{Injected } ^{14}\text{C}} \times 100$$

Measurement of the octanol/water partition coefficient

The partition coefficient for [¹²⁵I]5IA and [³H]nicotine was determined according to the previously reported method.⁴⁶ Briefly, a 10-μl aliquot of the sample was mixed with 3 ml each of 1-octanol and 0.1 M phosphate buffer in a test tube. The tube was shaken vigorously (3 × 1 min) and incubated for 20 min at room temperature, shaken and incubated again twice. After these procedures, the tube was centrifuged at 1,750 × g for 5 min at 4°C. Then 1-ml aliquots of each phase were removed, and the samples from [¹²⁵I]5IA were counted in a NaI well scintillation counter and those from [³H]nicotine were counted in a liquid scintillation counter.

Acute toxicity experiments

Male ICR mice weighing 28–32 g (five per group) were injected via the tail vein with one of three doses of 5IA: 0.1 μg/kg, 1 μg/kg or 10 g/kg. For 60 min after administration of 5IA, the pharmacological effects were observed.

SPECT studies of [¹²³I]5IA in the common marmoset

A male common marmoset (410 g) was first anesthetized intramuscularly with 20 mg/kg ketamine and 3mg/kg xylazine intramuscularly. Anesthesia was maintained throughout the study by intraperitoneal injection of sodium pentobarbital. The animal was placed in the SPECT bed and the head was restrained in a stereotaxic apparatus specifically designed for the SPECT scanner.

A two-scan protocol was used. In the control study, 300 MBq of [¹²³I]5IA was injected into the tail vein. For the displacement study, 6 mg/kg of (–)-cytisine was injected subcutaneously at 60 min after administration of [¹²³I]5IA (260 MBq). Sequential images of the brain were obtained over 4 hr with a SPECT-2000H scanner (Hitachi Medical Co., Tokyo, Japan) with specially designed pinhole collimators.⁴⁷ The energy window was symmetrical (± 10%), and centered on the iodine-123 photopeak (159 keV).

Images were reconstructed with a standard filtered back projection algorithm. Regions of interest (ROIs) were placed over different areas of the common marmoset brain with reference to a stereotaxic atlas and magnetic resonance imaging data. Radioactivity, expressed as counts per minute per ml, for each ROI was decay-corrected to the time of injection and corrected for the injected dose.

RESULTS

Chemistry

The precursor for radioiodination, *N*-*tert*-butoxycarbonyl (*N*-Boc)-protected tributylstannane (**7**), was synthesized in a two-step sequence (Fig. 2). First, Mitsunobu coupling of the 3-hydroxy-5-bromopyridine (**5**) with *N*-Boc-pro-

tected (*S*)-2-azetidinemethanol (**3**) gave *N*-Boc-protected 5-bromo analog of A-85380 (**6**) in 37% yield. Palladium-catalyzed stannyldibromination of the heteroaromatic ring gave **7** as a colorless oil in 58% yield.

Preparation of [¹²⁵I]5IA and [¹²³I]5IA (**11**) involved a two-step radiosynthetic sequence (Fig. 2). First, *N*-Boc-protected [^{123/125}I]5IA analog (**10**) was prepared in excellent radiochemical yield (> 80%) by an electrophilic iododestannylation reaction of *N*-Boc-protected tributylstannyl derivative (**7**). The second step of the reaction sequence involved removal of the *N*-Boc group of the radioiodinated 5IA analog (**10**) with hydrochloric acid to yield [^{123/125}I]5IA (**11**), which was purified by reverse-phase HPLC. The total radiochemical yield, after HPLC purification, was approximately 50%. The radiochemical purity of the product was greater than 98% as determined by HPLC, and the specific radioactivities of [¹²⁵I]5IA and [¹²³I]5IA were determined from the UV absorbance at 254 nm as more than 55 GBq/μmol (the limit of detection of this method). [¹²⁵I]5IA remained stable for at least one month at -20°C after labeling.

Unlabeled 5IA (**9**) was synthesized by iododestannylation of *N*-Boc-protected tributylstannane (**7**) with iodine monochloride, followed by deprotection of the *tert*-butoxycarbonyl protection group under acidic conditions, according to the method of Koren et al. with a slight

modification (10% yield).³⁶

In vitro binding

With the reference compounds A-85380, (-)-cytisine, (-)-nicotine and acetylcholine, we measured the affinity of 5IA for brain nicotine receptors by examining competition with [³H]cytisine for sites in rat cortical membranes. Table 1 summarizes K_i values determined from IC₅₀ of competitive binding curves of these compounds. 5IA showed very high binding affinity, which was the same as that of A-85380, 2.5-fold higher than that of (-)-cytisine and more than seven fold higher than that of (-)-nicotine. Furthermore, in competition assays with [¹²⁵I]5IA, A-85380 and (-)-cytisine, nicotinic agonists selective for the α4β2 subtype, inhibited the binding of [¹²⁵I]5IA, whereas α-bungarotoxin, an antagonist selective for the α7 subtype of nAChR, mecamylamine, a non-competitive nicotinic antagonist, and scopolamine, an antagonist at muscarinic acetylcholine receptors, did not inhibit the binding of [¹²⁵I]5IA (Table 2).

Lipophilicity

The lipophilicity of 5IA was assessed by *n*-octanol-phosphate buffer (pH 7.4) extraction. The partition coefficient of 5IA was lower than that of nicotine (log P; 5IA: 0.44 ± 0.01, nicotine: 1.36 ± 0.02) (mean ± S.D.).

Table 1 Inhibition of [³H]cytisine binding to rat brain membranes by various compounds

	K _i (nM)
5IA	0.37 ± 0.13
A-85380	0.38 ± 0.01
(-)-Cytisine	0.92 ± 0.42
(-)-Nicotine	2.71 ± 0.73
Acetylcholine	13.40 ± 2.61
Mecamylamine	> 100000
α-Bungarotoxin	> 100000

Each value represents the mean ± S.D. of three independent experiments.

Table 2 Inhibition of [¹²⁵I]5IA binding to rat cortical membranes by various compounds

	K _i (nM)
5IA	0.40 ± 0.13
(-)-Cytisine	1.40 ± 0.47
(-)-Nicotine	1.32 ± 0.25
Acetylcholine	41.4 ± 1.80
Scopolamine	> 100000
Spiperone	> 100000
α-Bungarotoxin	> 100000
Mecamylamine	> 100000

Each value represents the mean ± S.D. of three independent experiments.

Table 3 Biodistribution of radioactivity after administration of [¹²⁵I]5IA in rats^{a)}

	Time after injection (min)					
	5	15	30	60	120	180
Blood	0.24 ± 0.02	0.23 ± 0.02	0.21 ± 0.01	0.14 ± 0.02	0.14 ± 0.01	0.15 ± 0.01
Liver	1.34 ± 0.13	1.71 ± 0.13	1.50 ± 0.11	1.55 ± 0.08	0.77 ± 0.09	0.88 ± 0.14
Kidney	3.06 ± 0.22	3.86 ± 0.56	4.93 ± 0.73	5.09 ± 1.14	1.79 ± 0.62	1.15 ± 0.14
Heart	0.49 ± 0.04	0.30 ± 0.03	0.22 ± 0.01	0.19 ± 0.01	0.07 ± 0.01	0.07 ± 0.01
Thyroid ^{b)}	0.02 ± 0.004	0.05 ± 0.01	0.16 ± 0.03	0.44 ± 0.14	1.95 ± 0.44	2.39 ± 0.43
Brain	0.61 ± 0.06	0.73 ± 0.07	0.87 ± 0.09	1.05 ± 0.13	0.66 ± 0.04	0.71 ± 0.01
Br/Bl ^{c)}	2.41 ± 0.12	3.08 ± 0.36	4.09 ± 0.57	7.89 ± 1.45	4.78 ± 0.39	4.49 ± 0.30

^{a)} Percent of injected ¹²⁵I dose/g of organ; the mean ± S.D. for four rats. ^{b)} Percent of injected ¹²⁵I dose/organ; the mean ± S.D. for four rats. ^{c)} Br/Bl = Brain-to-blood ratio (percent of injected ¹²⁵I dose/g of tissue ratio).

Brain uptake index

The penetration of 5IA across the blood-brain barrier was assessed by the brain uptake index (BUI). 5IA had a moderate BUI (31 ± 6), which was lower than that of nicotine (103 ± 12) (mean \pm S.D.).

Biodistribution in rats

The biodistribution of radioactivity after intravenous injection of [125 I]5IA is shown in Table 3. Marked accumulation of radioactivity in the brain was seen with time after injection and the peak concentration was observed at 60 min, declining gradually over the next 120 min. The radioactivity in blood was cleared rapidly, and the highest brain-to-blood ratio of 7.5 was obtained at 60 min after injection. High uptake was observed in the kidneys, which was cleared rapidly after 60 min. The liver showed moderate initial uptake and a gradual decrease with time. Uptake in the thyroid was low during the early phase and gradually increased with time, but was not particularly high (0.44 ± 0.14 , 1.95 ± 0.44 , $2.39 \pm 0.43\%$ injected dose/organ at 60, 120, 180 min, respectively) (mean \pm S.D.).

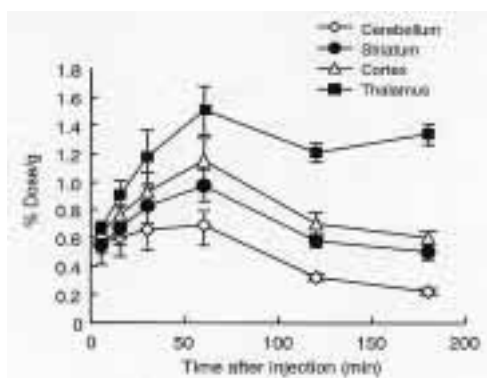


Fig. 3 Regional brain uptake of [125 I]5IA in rats. Each point represents the mean \pm S.D. for four rats.

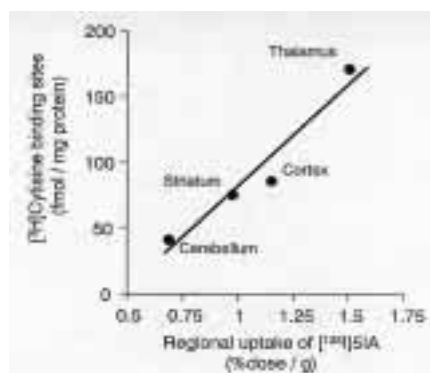


Fig. 4 Correlation between radioactivity levels determined from the *in vivo* regional distribution of [125 I]5IA at 60 min postinjection in rats and density of nicotinic cholinergic receptor sites as determined by *in vitro* [3 H]cytisine binding.

The temporal distribution profile of the radioactivity in various rat brain regions is shown in Figure 3. Differences in the regional distribution of radioactivity were observed. At 60 min after injection, the highest concentration of radioactivity was detected in the thalamus, followed by moderate uptake in the cortex and striatum. Cerebellar accumulation was the lowest. The regional distribution paralleled the distribution of nAChRs determined by *in vitro* studies.^{22,36} Furthermore, different rates of radioactivity clearance were noted in the various brain regions. For example, clearance of radioactivity in the thalamus was relatively slow from 60 min to 180 min, but that in the cerebellum was rather rapid. Therefore, region to cerebellum ratios progressively increased over 180 min, with the most dramatic changes occurring in the thalamus, attaining a value of 6.3. The regional distribution of [125 I]5IA at 60 min postinjection correlated well with the known distribution of nAChRs determined by *in vitro* receptor assay⁴² ($\gamma = 0.97$) (Fig. 4). Moreover, the effects of various drugs on the levels of [125 I]5IA in various brain regions were studied. In these experiments, the uptake of radioactivity in brain regions was measured at 60 min and compared to that of saline-treated controls. As shown in Figure 5, the administration of cytisine, (-)-nicotine and 5IA, drugs with high affinity for nAChR, significantly reduced the uptake of radioactivity in all regions, and resulted in similar levels of radioactivity throughout the brain. In particular, the reduction in the radioactivity level was most pronounced in the thalamus with a reduction of more than 85%. The administration of (+)-nicotine with lower affinity for nAChR moderately

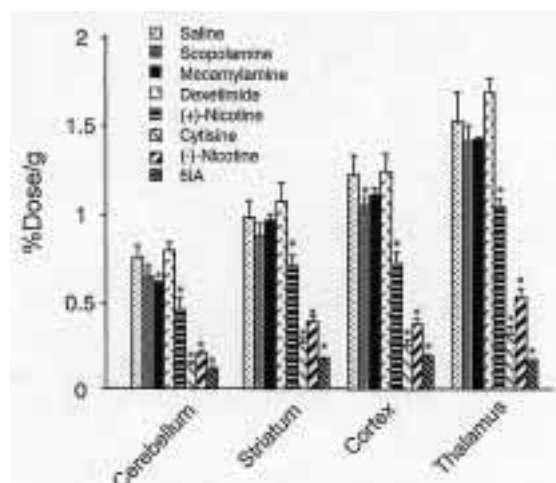


Fig. 5 Effects of various drugs on the regional uptake of [125 I]5IA in rats 60 min after injection. [125 I]5IA was intravenously injected 5 min after intravenous administration of cytisine (1 mg/kg), (-)-nicotine (60 μ g/kg), (+)-nicotine (0.3 mg/kg), dexametide (10 mg/kg), 5IA (0.1 mg/kg) and saline, and 30 min after subcutaneous administration of scopolamine (10 mg/kg) and mecamylamine (5 mg/kg). * $p < 0.01$ as compared with saline control group (Dunnett's multiple comparisons test).

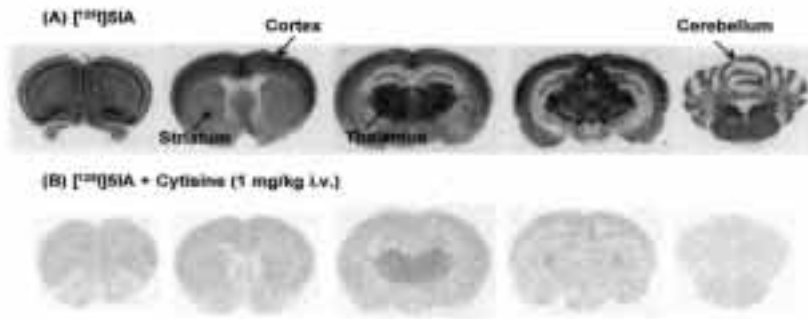


Fig. 6 *Ex vivo* autoradiograms of rat coronal brain sections at 60 min after injection of [¹²⁵I]5IA. (A) [¹²⁵I]5IA alone and (B) cytisine (1 mg/kg) administered 5 min before [¹²⁵I]5IA injection.

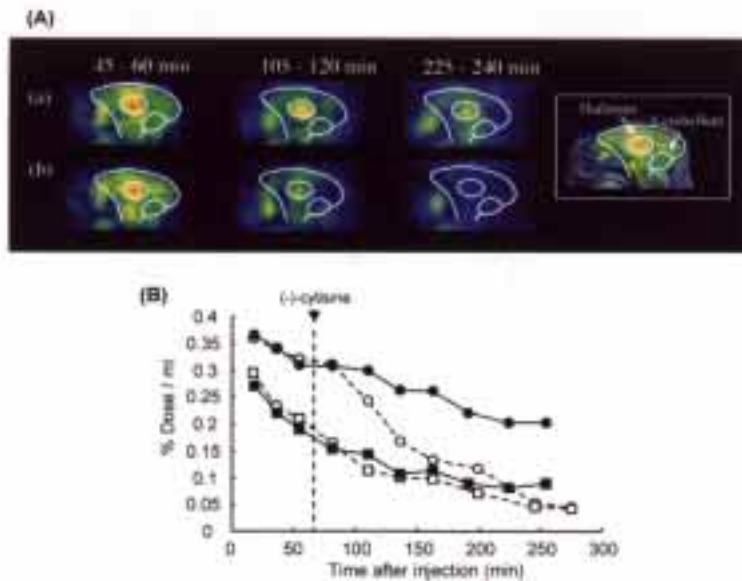


Fig. 7 (A) Sagittal SPECT images and (B) time-radioactivity curves of [¹²³I]5IA in the common marmoset brain. (–)-Cytisine (6 mg/kg s.c.) was administered 60 min after [¹²³I]5IA injection. (A) The figure on the right shows a SPECT image superposed on MRI images. Time on each figure is the time after injection of [¹²³I]5IA. (B) □ : thalamus in control study, ○ : cerebellum in control study, ■ : thalamus in (–)-cytisine displacement study, ● : cerebellum in (–)-cytisine displacement study.

reduced the uptake of radioactivity. Dexametidine and scopolamine, drugs with high selective affinity for muscarinic acetylcholine receptors, caused no changes in the accumulation. Similar negative results were observed for rats treated with mecamylamine, a non-competitive nicotinic antagonist. None of the compounds tested showed any effect on the radioactivity in the blood.

Ex vivo autoradiographic studies in the rat brain were in agreement with the results of the biodistribution studies described above. Figure 6A shows the autoradiograms of [¹²⁵I]5IA in rat brain sections at 60 min postinjection. The highest level of accumulation of radioactivity was observed in the thalamus. Figure 6B shows the effects of (–)-cytisine on radioligand brain distribution. Binding of [¹²⁵I]5IA throughout the brain was nearly completely

inhibited by treatment of (–)-cytisine.

Metabolism

Analysis of brain homogenates was carried out at various intervals until 60 min after injection of [¹²⁵I]5IA in rats. Approximately 90% of the radioactivity in the homogenate could be extracted with methanol and the methanol-extracted fraction displayed a single peak on HPLC with the same retention time as that of unlabeled 5IA at all tested times.

Blood samples were also taken at various times after [¹²⁵I]5IA injection in rats and analyzed by HPLC. HPLC analyses revealed a high level of the original compound in the early period, but its relative contribution to total blood radioactivity declined sharply with time; i.e. the amounts

of unchanged [125 I]5IA were 90 ± 9 , 60 ± 8 , 18 ± 5 , 13 ± 5 and $3 \pm 1\%$ (mean \pm S.D., $n = 4$), respectively, at 2, 5, 15, 30 and 60 min postinjection. The radioactivity other than [125 I]5IA was attributable mainly to two more hydrophilic metabolites with shorter retention times in the reverse-phase column.

Acute toxicity experiments

Three different doses of unlabeled 5IA ranging from 0.1 $\mu\text{g}/\text{kg}$ to 10 $\mu\text{g}/\text{kg}$ were intravenously injected in separate groups of mice to gauge the acute toxicity of this ligand. No convulsions or death were observed in any animals studied although the temporary decrease in locomotor activity that was undetectable 30 min after injection was observed in mice treated with a 10 $\mu\text{g}/\text{kg}$ dose.

SPECT imaging in the common marmoset

Figure 7 shows SPECT images of a common marmoset at 45–60, 105–120 and 225–240 min, and time-radioactivity curves in the thalamus and cerebellum after intravenous injection of [123 I]5IA. After injection of [123 I]5IA, there was a rapid and high level of accumulation of radioactivity in the brain. Soon after injection, the radioactivity was distributed according to the regional cerebral blood flow, but the elimination rate was different in the various regions, and therefore a noticeably heterogeneous distribution of radioactivity was observed after 60 min, with the highest levels observed in the thalamus, intermediate levels in the cortex, and lowest levels in the cerebellum. Treatment with cytosine (6 mg/kg, subcutaneous) 60 min after injection of the radioligand accelerated the elimination rate in the thalamus and cortex, but not in the cerebellum. At 180 min after cytosine administration, radioactivity was reduced by 74% in the thalamus in comparison with the control study and nearly identical levels of radioactivity were observed in all brain regions.

DISCUSSION

Recently, Koren et al. reported that 5IA shows high affinity for central nAChRs *in vitro* and *in vivo* and [123 I]5IA is a promising SPECT imaging agent of nAChRs.^{36–41} Furthermore, our previous study of the structure-activity relationship in nicotine derivatives has supported the potentiality of 5IA as a radioligand for nAChR study.^{19,20,37} In the present study, *in vitro* and *in vivo* studies were performed to evaluate the clinical applicability of [123 I]5IA as a radiopharmaceutical for SPECT studies of central nAChRs.

In vitro receptor binding studies showed that 5IA had the same high receptor affinity as the parent compound, A-85380 (Table 1). Furthermore, in competition assays with [125 I]5IA, A-85380 and (–)-cytosine, nicotinic agonists selective for the $\alpha 4\beta 2$ subtype,^{32,48} inhibited the binding of [125 I]5IA, whereas α -bungarotoxin, an antagonist selective for the $\alpha 7$ subtype of nAChR,⁴⁹ meca-

mylamine, a non-competitive nicotinic antagonist, and scopolamine, an antagonist at muscarinic acetylcholine receptors, did not inhibit the binding of [125 I]5IA (Table 2). Results of the competition assay indicated the high selectivity of 5IA for the $\alpha 4\beta 2$ nAChR subtype. The excellent affinity and selectivity of 5IA for the central $\alpha 4\beta 2$ nAChR subtype is in agreement with the results of other groups.^{32,36,41,48}

A simple oxidant-promoted electrophilic iododestannylation reaction offers several advantages for radioiodination, since it is performed under very mild conditions and with very high regional selectivity, as well as affording a high specific radioactivity. For radiosynthesis of [$^{123/125}$ I]5IA (**11**) from compound **7**, we therefore tried two methods which employ electrophilic radioiododestannylation reaction. In our first efforts at the preparation of [$^{123/125}$ I]5IA, we synthesized an *N*-deprotected tri-butylstannyl derivative by removing the *N*-Boc group and then performed the radioiododestannylation reaction (method A), since this required only one step of treatment with radioiodine. But subsequent experiments revealed that the reaction sequence of radioiododestannylation followed by deprotection (method B) gave higher total radiochemical yields (approximately 50%) than method A (approximately 15%) since the radiochemical yield of the radioiododestannylation of *N*-deprotected tri-butylstannyl derivative was low. These results indicated that method B is preferable to method A for routine radiosynthesis of [$^{123/125}$ I]5IA. Musachio et al. and Hori et al. also synthesized [123 I]5IA by method B in the almost same yield as ours although, as an oxidizing agent, chloramines T was used instead of hydrogen peroxide,^{40,41} indicating that the type of oxidizing agent does not affect the yield of this iododestannylation reaction.

The biodistribution of [125 I]5IA was evaluated in rats since there are many useful models in rats for various neurodegenerative disorders.⁵⁰ High accumulation in the brain was observed; i.e. the radioactivity in the brain increased sharply with time after injection and the peak level in the brain was reached at 60 min, showing an increase by a factor of 1.7 as compared with that at 5 min (Table 3). By comparison, (–)-[^{11}C]nicotine enters the brain rapidly with peak levels occurring soon after injection, whereas after 30 min only 30% of the maximal activity remains.⁵¹ The slightly lower initial uptake and slower uptake kinetics of 5IA by the brain may be responsible for the lower BUI than (–)-nicotine (% of injected dose at 5 min after injection; 1.1% for 5IA, 2.3% for (–)-nicotine) (BUI; 31 for 5IA, 103 for (–)-nicotine).

Studies of the regional brain distribution of [125 I]5IA showed high accumulation of radioactivity in the thalamus, intermediate in the cortex and striatum, and lowest in the cerebellum (Fig. 3). This regional distribution was correlated well with the distribution of nAChRs determined by *in vitro* receptor assay (Fig. 4).^{22,42,52,53} Moreover, brain uptake of [125 I]5IA was significantly blocked

by nAChR agonists, (–)-nicotine and (–)-cytisine, but scopolamine or dexetimide, competitive antagonists at muscarinic acetylcholine receptors, or mecamylamine, a blocker of nAChR channels, did not influence the accumulation of [¹²⁵I]5IA in the brain (Fig. 5). Injection of unlabeled 5IA (0.1 mg/kg) resulted in an approximately 90% reduction in radiotracer accumulation in the thalamus. This finding demonstrated the saturability of the sites labeled with the [¹²⁵I]5IA and the low level of nonspecific binding *in vivo*. These results on selectivity and saturability indicated that 5IA binds to nAChRs in the brain after intravenous injection. The selectivity and saturability of cerebral distribution of radioiodinated 5IA have also been reported recently in mice by other groups.^{36,39,40} Autoradiographic studies were consistent with these results (Fig. 6). Furthermore, HPLC analysis of brain homogenates after injection of [¹²⁵I]5IA showed that a large percentage were in the original form, indicating that the distribution of radioactivity was based on intact 5IA and more polar radiolabeled metabolites present in the blood were unable to penetrate the blood-brain barrier.

Imaging studies with SPECT were carried out in the common marmoset which is a kind of ease-treated small monkey and showed [¹²³I]5IA to be a highly specific radiopharmaceutical for *in vivo* investigations of central nAChRs (Fig. 7). [¹²³I]5IA exhibited a regional localization consistent with the known densities of nAChRs ($\alpha 4\beta 2$ subtype) in primates (thalamus > cortical regions > cerebellum).⁵² [¹²³I]5IA uptake could be displaced by treatment with (–)-cytisine, a well-characterized nAChR agonist, demonstrating that specific binding of [¹²³I]5IA to central nAChRs can be visualized via SPECT imaging and that the binding of [¹²³I]5IA to nAChR sites was reversible. Furthermore, since the accumulation in the cerebellum, which showed the lowest level of radioactivity in the brain, was not influenced by treatment with (–)-cytisine, SPECT imaging studies demonstrated that this region could be used as an indicator of nonspecific binding.

Furthermore, 5IA has a greatly reduced toxicity profile relative to other nAChR antagonists such as epibatidine and (–)-nicotine. For example, whereas the 2-fluorinated analog of epibatidine produces lethality (30%) at an intravenous dose of 1.5 $\mu\text{g}/\text{kg}$,⁵⁴ no behavioral effects were observed in our preliminary pharmacological study when 0.1–10 $\mu\text{g}/\text{kg}$ of 5IA was administered intravenously to mice. These results therefore indicated that 5IA is nontoxic at concentrations about three to six thousand-fold higher than that predicted for imaging receptors in man (1.5–3 ng/kg). The lower toxicity of 5IA might be associated with its low affinity at $\alpha 3\beta 4$ receptors, another nAChR subtype in the brain, to which epibatidine binds with high affinity.^{55,56}

In conclusion, gathered results indicate that 5IA has very high affinity and selectivity for the central $\alpha 4\beta 2$

nAChR subtype. Furthermore, 5IA showed high brain uptake, regional cerebral distribution in association with nAChRs and low toxicity. In addition, [¹²³I]5IA allowed visualization of central nAChR sites in the common marmoset by SPECT. [¹²³I]5IA therefore appears promising for human imaging studies of central nAChRs in normal and disease states.

ACKNOWLEDGMENTS

This work was supported in part by a grant from the “Research for the Future” Program of the Japan Society for the promotion of Science (JSPS-RFTF97K00201), grants-in-aid for Scientific Research from the Ministry of Education, Science and Technology of Japan, a research grant for Longevity Sciences from the Ministry of Health and Welfare, and a grant for the Smoking Research Foundation. The authors thank Nihon Medi-Physics Co. Ltd., Japan, for providing ammonium [¹²³I]iodide and Sumitomo Chemical Co. Ltd., Japan, for supplying a common marmoset.

REFERENCES

1. Norberg A, Winbald B. Reduced number of [³H]nicotine and [³H]acetylcholine binding sites in the frontal cortex of Alzheimer brains. *Neurosci Lett* 1986; 72: 115–119.
2. Whitohouse PJ, Martino AM, Antuono PG, Lowenstein PR, Coyle JT, Price DL, et al. Nicotinic acetylcholine binding sites in Alzheimer’s disease. *Brain Res* 1986; 371: 146–151.
3. Kellar KJ, Whitehouse PJ, Martino-Barrows AM, Marcus K, Price DL. Muscarinic and nicotinic cholinergic binding sites in Alzheimer’s disease cerebral cortex. *Brain Res* 1987; 436: 62–68.
4. Whitohouse PJ, Martino AM, Wagster MV, Price DL, Mayeux L, Atack JR, et al. Reductions in [³H]-nicotinic acetylcholine binding in Alzheimer’s disease and Parkinson’s disease: an autoradiographic study. *Neurology* 1988; 38: 720–723.
5. Whitohouse PJ, Martino AM, Marcus KA, Zweig RM, Singer HS, Price DL, et al. Reductions in acetylcholine and nicotine binding in several degenerative diseases. *Arch Neurol* 1988; 45: 722–724.
6. London ED, Ball MJ, Waller SB. Nicotinic binding sites in cerebral cortex and hippocampus in Alzheimer’s dementia. *Neurochem Res* 1989; 14: 745–750.
7. Rinne JO, Myllykyla R, Lonnberg P, Marjamaki P. A postmortem study of brain nicotinic receptors in Parkinson’s and Alzheimer’s disease. *Brain Res* 1991; 547: 167–170.
8. Giacobini E. Nicotinic cholinergic receptors in human brain: effects of aging and Alzheimer. *Adv Exp Med Biol* 1991; 296: 303–315.
9. Gotti C, Fornasari D, Clementi F. Human neuronal nicotinic receptors. *Prog Neurobiol* 1997; 53: 199–237.
10. Warpman U, Nordberg A. Epibatidine and ABT 418 reveal selective losses of $\alpha 4\alpha 2$ nicotinic receptors in Alzheimer brains. *Neuro Report* 1995; 6: 2419–2423.
11. Benewell MEM, Balfour DJK, Anderson JM. Evidence that tobacco smoking increases the density of (–)-[³H]nicotine binding sites in human brain. *J Neurochem* 1988; 50: 1243–

- 1247.
12. Yates SL, Bencherif M, Fluhler EN, Lippiello PM. Upregulation of nicotinic acetylcholine receptors following chronic exposure of rats to mainstream cigarette smoker or $\alpha 2$ receptors to nicotine. *Biochem Pharmacol* 1995; 50: 2001–2008.
 13. Breese CR, Marks MJ, Logel J, Adams CE, Sullivan B, Collins AC, et al. Effect of smoking history on [^3H]nicotine binding in human postmortem brain. *J Pharmacol Exp Ther* 1997; 282: 7–13.
 14. Irle E, Markowitsch HJ. Basal forebrain-lesioned monkeys are severely impaired in tasks of association and recognition memory. *Ann Neurol* 1985; 14: 1025–1032.
 15. Decker MW, Brioni JD, Bannon AW, Arneric SP. Diversity of neuronal nicotinic acetylcholine receptors: lessons from behavior and implications for CNS therapeutics. *Life Sci* 1995; 56: 545–570.
 16. Levin ED, Rose JE. Acute and chronic nicotinic interactions with dopamine systems and working memory performance. *Ann NY Acad Sci* 1995; 757: 245–252.
 17. Jones S, Sudweeks S, Yakel JL. Nicotinic receptors in the brain: correlating physiology with function. *Trends Neurosci* 1999; 22: 555–561.
 18. Kenneth Lloyd G, Williams M. Neuronal nicotinic acetylcholine receptors as novel drug targets. *J Pharmacol Exp Ther* 2000; 292: 461–467.
 19. Saji H, Watanabe A, Kiyono Y, Magata Y, Iida Y, Takaishi Y, et al. Application of [^{125}I](S)-5-iodonicotine, a new radioiodinated ligand, in the assay of nicotinic acetylcholine receptor binding in the brain. *Biol Pharm Bull* 1995; 18: 1463–1466.
 20. Saji H, Watanabe A, Magata Y, Ohmomo Y, Kiyono Y, Yamada Y, et al. Synthesis and characterization of radioiodinated (S)-5-iodonicotine: a new ligand for potential imaging of brain nicotinic cholinergic receptors by single photon emission computed tomography. *Chem Pharm Bull* 1997; 45: 284–290.
 21. Badio B, Daly JW. Epibatidine, a potent analgetic and nicotinic agonist. *Mol Pharmacol* 1994; 45: 563–569.
 22. Houghtling RA, Davila-Garcia MI, Kellar KJ. Characterization of (\pm)-[^3H]epibatidine binding to nicotinic cholinergic receptors in rat and human brain. *Mol Pharmacol* 1995; 48: 280–287.
 23. Perry DC, Kellar KJ. ^3H -epibatidine labels nicotinic receptors in rat brain: an autoradiographic study. *J Pharmacol Exp Ther* 1995; 275: 1030–1034.
 24. London ED, Scheffel U, Kimes AS, Kellar KJ. *In vivo* labeling of nicotinic acetylcholine receptors in the brain with [^3H]epibatidine. *Eur J Pharm* 1995; 278: R1–R2.
 25. Scheffel U, Taylor GF, Kepler JA, Carroll FI, Kuhar MJ. *In vivo* labeling of neuronal nicotinic acetylcholine receptors with radiolabeled isomers of norchloroepibatidine. *NeuroReport* 1995; 6: 2483–2488.
 26. Horti AG, Ravert HT, London ED, Dannals RF. Synthesis of a radiotracer for studying nicotinic acetylcholine receptors by positron emission tomography: (\pm)-exo-2-(2-[^{18}F]fluoro-5-pyridyl)7-azabicyclo[2.2.1]heptane. *J Labell Comp Radiopharm* 1996; 38: 355–366.
 27. Horti AG, Scheffel U, Stathis M, Finley P, Ravert HT, London ED, et al. Fluorine-18-FPH for PET imaging of nicotinic acetylcholine receptors. *J Nucl Med* 1997; 38: 1260–1265.
 28. Villemagne VL, Horti AG, Scheffel U, Ravert HT, Finley P, Clough DJ, et al. Imaging nicotinic acetylcholine receptors with Fluorine-18-FPH, an epibatidine analog. *J Nucl Med* 1997; 38: 1737–1741.
 29. Horti A, Scheffel U, Kimes AS, Musachio JL, Ravert HT, Mathews WB, et al. Synthesis and evaluation of [^{11}C]-N-methylated analogs of epibatidine as tracers for PET studies of nicotinic acetylcholine receptors. *J Med Chem* 1998; 41: 4199–4206.
 30. Musachio JL, Villemagne VL, Scheffel U, Stathis M, Finley P, Horti AG, et al. [$^{125/123}\text{I}$]IPH: a radioiodinated analog of epibatidine for *in vivo* studies of nicotinic acetylcholine receptors. *Synapse* 1997; 26: 392–399.
 31. Musachio JL, Horti AG, London ED, Dannals RF. Synthesis of a radioiodinated analog of epibatidine: (\pm)-exo-2-(2-iodo-yrityl)7-azabicyclo[2.2.1]heptane for *in vitro* and *in vivo* studies of nicotinic acetylcholine receptors. *J Labell Comp Radiopharm* 1997; 39: 39–48.
 32. Abreo MA, Lin NH, Garvey DS, Gunn ED, Hettinger AM, Wasicak JT, et al. Novel 3-Pyridyl ethers with subnanomolar affinity for central neuronal nicotinic acetylcholine receptors. *J Med Chem* 1996; 39: 817–825.
 33. Sheridan RP, Nilakantan R, Dixon JS, Venkataraghavan R. The ensemble approach to distance geometry: application to the nicotinic pharmacophore. *J Med Chem* 1986; 29: 899–906.
 34. Barlow RB, Johnson O. Relations between structure and nicotine-like activity: X-ray crystal structure analysis of (–)-cytidine and (–)-lobeline hydrochloride and a comparison with (–)-nicotine and other nicotine-like compounds. *Br J Pharmacol* 1989; 98: 799–808.
 35. Glennon RA, Dukat M. Nicotinic cholinergic receptor pharmacophores. In: *Neuronal Nicotinic Receptors: Pharmacology and Therapeutic Opportunities*. Arneric SP, Brioni JD (eds), New York; Wiley-Liss, 1999: 271–284.
 36. Koren AO, Horti AG, Mukhin AG, Gundisch D, Kimes AS, Dannals RF, et al. 2-, 5-, and 6-Halo-3-(2(S)-azetidinylmethoxy)pyridines: synthesis, affinity for nicotinic acetylcholine receptors, and molecular modeling. *J Med Chem* 1998; 41: 3690–3698.
 37. Vaupel DB, Mukhin AG, Kimes AS, Horti AG, Koren AO, London ED. *In vivo* studies with [^{125}I]-5-I-A-85380, a nicotinic acetylcholine receptor radioligand. *NeuroReport* 1998; 9: 2311–2317.
 38. Musachio JL, Scheffel U, Finley PA, Zhan Y, Michizuki T, Wagner Jr HN, et al. 5-[I-125/123]Iodo-3(2(S)-azetidinylmethoxy)pyridine, a radioiodinated analog of A-85380 for *in vivo* studies of central nicotinic acetylcholine receptors. *Life Sci* 1998; 62: 351–357.
 39. Chefer SI, Horti AG, Lee KS, Koren AO, Jones DW, Gorey JG, et al. *In vivo* imaging of brain nicotinic acetylcholine receptors with 5-[^{123}I]iodo-A-85380 using single photon emission computed tomography. *Life Sci* 1998; 63: 355–360.
 40. Musachio JL, Villemagne VL, Scheffel UA, Dannals RF, Dagan AS, Yokoi F, et al. Synthesis of an I-123 analog of A-85380 and preliminary SPECT imaging of nicotinic receptors in baboon. *Nucl Med Biol* 1999; 26: 201–207.
 41. Horti AG, Koren AO, Lee KS, Mukhin AG, Vaupel DB, Kimes AS, et al. Radiosynthesis and preliminary evaluation of 5-[$^{123/125}\text{I}$]iodo-3(2(S)-azetidinylmethoxy)pyridine: a

- radioligand for nicotinic acetylcholine receptors. *Nucl Med Biol* 1999; 26: 175–182.
42. Pabreza LA, Dhawan S, Kellar KJ. [³H]cytisine binding to nicotinic cholinergic receptors in brain. *Mol Pharmacol* 1991; 39: 9–12.
 43. Lowry OH, Rosebrough NJ, Farr AL, Randall RJ. Protein measurement with the Folin phenol reagent. *J Biol Chem* 1951; 193: 265–275.
 44. Cheng Y, Prusoff WH. Relationship between the inhibition constant (K_i) and the concentration of inhibitor which causes 50 per cent inhibition (IC_{50}) of an enzymatic reaction. *Biochem Pharmacol* 1973; 22: 3099–3108.
 45. Oldendorf WH. Measurement of brain uptake of radiolabeled substances using a tritiated water internal standard. *Brain Res* 1970; 24: 372–376.
 46. Saji H, Iida Y, Nakatsuka I, Kataoka M, Ariyoshi K, Magata Y, et al. Radioiodinated 2'-iododiazepam: a potential imaging agent for SPECT investigations of benzodiazepine receptors. *J Nucl Med* 1993; 34: 932–937.
 47. Ishizu K, Mukai T, Yonekura Y, Pagani M, Fujita T, Magata Y, et al. Ultra-high resolution SPECT system using four pinhole collimators for small animal studies. *J Nucl Med* 1995; 36: 2282–2287.
 48. Mukhin AG, Gundisch D, Horti AG, Koren AO, Tamagnan G, Kimes AS, et al. 5-iodo-A-85380, an $\alpha 4\beta 2$ subtype-selective ligand for nicotinic acetylcholine receptors. *Mol Pharmacol* 2000; 57: 642–649.
 49. Del Toro E, Juiz J, Peng X, Lindstrom J, Criado M. Immunocytochemical localization of the $\alpha 7$ subunit of the nicotinic acetylcholine receptor in the rat central nervous system. *J Comp Neurol* 1994; 349: 325–342.
 50. Kawamata J, Matusita H. *Shikkan Moderu Doubutu Handobukku*, Tokyo, 1982.
 51. Saji H, Magata Y, Yamada Y, Tajima K, Yonekura Y, Konishi J, et al. Synthesis of (*S*)-*N*-[methyl-¹¹C]nicotine and its regional distribution in the mouse brain: a potential tracer for visualization of brain nicotinic receptors by positron emission tomography. *Chem Pharm Bull* 1992; 40: 734–736.
 52. Norberg A, Alafuzoff I, Winblad B. Nicotinic and muscarinic subtypes in the human brain: changes with aging and dementia. *J Neurosci Res* 1992; 31: 103–111.
 53. Fleisher JE, Scheffel U, London ED, Frost JJ. *In vivo* labeling of nicotinic cholinergic receptors in the brain with [³H]cytisine. *Life Sci* 1994; 54: 1883–1890.
 54. Molina PE, Ding YS, Carroll FI, Liang F, Volkow ND, Pappas N, et al. Fluoro-norchloroepibatidine: preclinical assessment of acute toxicity. *Nucl Med Biol* 1997; 24: 743–747.
 55. Studerman KA, Mahaffy LS, Akong M, Velicebebi G, Chavez-Noriega LE, Crona JH, et al. Characterization of human recombinant neuronal nicotinic acetylcholine receptor subunit combinations $\alpha 2\beta 4$, $\alpha 3\beta 4$ and $\alpha 4\beta 4$ stably expressed in HEK293 cells. *J Pharmacol Exp Ther* 1998; 284: 777–789.
 56. Xiao Y, Meyer EL, Thompson JM, Surin A, Wroblewski J, Kellar KJ. Rat $\alpha 3/\beta 4$ subtype of neuronal nicotinic acetylcholine receptor stably expressed in a transfected cell line: pharmacology of ligand binding and function. *Mol Pharmacol Exp Ther* 1998; 54: 322–333.